Magneto-optical Effects Enhanced by Surface Plasmons in Metallic Multilayer Films

V. I. Safarov, V. A. Kosobukin,* C. Hermann, G. Lampel, and J. Peretti

Laboratoire de Physique de la Matière Condensée, Ecole Polytechnique, 91128 Palaiseau Cedex, France

C. Marlière

Institut d'Optique Théorique et Appliquée, Centre Universitaire, Bâtiment 503, 91403 Orsay Cedex, France
(Received 27 May 1994)

Magneto-optical properties of noble-metal–ferromagnetic-metal multilayer thin films have been investigated in the total reflection condition. The experimental and theoretical study of a Au/Co/Au model structure demonstrates that the resonant coupling of the p component of the light electric field with the gold surface plasmons results in an enhancement of the magneto-optical response of the system, both in the reflected light and in the evanescent mode.

Very thin ferromagnetic layers embedded in metallic matrices have received a lot of attention in the past few years because of their specific physical properties, such as perpendicular magnetization, giant magnetoresistive, and magneto-optical (MO) effects [1], which are very attractive both for fundamental physics studies and technological applications.

In the variety of systems which are now available, the quality of the interfaces and of the crystalline structure as well as their magnetic properties may be controlled, in particular by properly choosing the matrix materials. Noble metals are generally suitable for these applications. In another respect, noble metals have specific electronic and optical properties which may be used to improve MO responses. Thus, in ferromagnetic-metal/noble-metal multilayer structures, enhancement of polar Kerr rotations have been observed at the bulk plasmon edge of the noble-metal dielectric function $\varepsilon(\omega)$ [2]. The detailed interpretation of the effect of bulk plasmons on MO properties, which was also reported for ferromagnetic crystals [3], still remains controversial [4]. Electronic resonances of another type, which are very strong in noble metals, are the surface plasmon modes [5]. These coherent charge oscillations propagating along a metal surface can be excited, in a wide spectral range, by the p component of the evanescent light electric field when the sample is illuminated in total reflection condition. Up to now, the data reported in the literature on the influence of surface plasmons on Kerr effect concern ferromagnetic metals [6], where surface plasmon resonances are not well defined due to overdamping ($|\mathrm{Re}(\varepsilon)/\mathrm{Im}(\varepsilon)| < 1$).

In the present Letter, we report a precise analysis of the MO properties, in total reflection geometry, of a model Au/Co/Au multilayer structure where the well-defined noble-metal surface plasmon resonance, of high quality factor ($|\mathrm{Re}(\varepsilon)/\mathrm{Im}(\varepsilon)| \gg 1$), can be excited. Our experimental and theoretical results show that, in this case, a resonancelike characteristic feature is observed in the MO response both in the reflected beam and in the *evanescent mode* close to the film surface. This feature actually corresponds to a strong enhancement of the MO figure of merit of the whole system.

We have designed a magneto-optics experiment operating in total reflection geometry, with polarization sensitive detection of the evanescent mode and of the reflected light (Fig. 1). The $d = 30$ nm thick Au/Co/Au film is grown on a glass plate under UHV conditions [7]. The thickness of the substrate and cap gold layers are, respectively, $d' = 25$ nm and $d'' = 4$ nm. The $\ell = 1$ nm thick cobalt layer has its easy-magnetization axis perpendicular to the film plane and exhibits a square hysteresis loop. The glass plate is optically coupled to a half-cylindrical glass prism with adapting refractive index liquid. Linearly polarized light of wavelength 647 nm (the red line of a Kr^+ laser) illuminates the sample through the prism at a variable incident angle θ. The intensity and polarization of the reflected beam are analyzed. For the θ values beyond the total reflection limit, the evanescent mode close to the sample surface is collected by a tip-ending monomode optical fiber which guides the light to a photomultiplier tube equipped with a polarization analyzer. The tip is mounted on a scanning tunneling optical microscope [8] head. The characteristics and performances of this polarization-sensitive microscope are described in detail elsewhere [9].
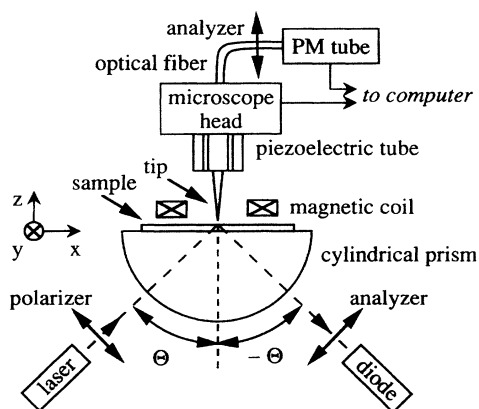

FIG. 1.   Schematics of the magneto-optics experiment setup.

The MO effects in the reflected beam and in the evanescent mode are measured by means of specific modulation techniques. In pulsed-current operation, a small coil surrounding the tip delivers alternating (at 20 Hz) 10 μs long pulses of magnetic field perpendicular to the film plane and larger than the Co-layer coercive field (≈ 1 kOe) without perturbing near-field measurements. This way, the saturated magnetization of the Co layer is periodically flipped at 20 Hz. The modulation of the light polarization induced by the MO effect, at this frequency, is detected as an intensity modulation through a linear analyzer oriented at 45° to the incident polarization axis. The ac component of the detector output signal at the modulation frequency, measured through a lock-in amplifier, is the MO signal Σ_{MO} (i.e., the amplitude of the MO hysteresis loop at zero external magnetic field). In near-field measurements, the dc component of the detector output signal is used in the feedback loop of the tip-to-sample distance to maintain a constant average detected intensity.

For linearly polarized incident light, the MO effect can be considered as the appearance of a component perpendicular to the incident polarization direction. When the light is initially s (p) polarized, the detected electric field has then two perpendicular components, $\mathbf{E}^s$ ($\mathbf{E}^p$) related to the incident light electric field and $\mathbf{E}^p$ ($\mathbf{E}^s$) magneto-optically induced. Therefore, for both excitation polarizations, the expression for Σ_{MO} is

$$\Sigma_{MO} = |E^p(\theta)|\,|E^s(\theta)|\cos[\Delta\phi(\theta) + \psi], \qquad (1)$$

where E^s and E^p are the amplitudes of $\mathbf{E}^s$ and ($\mathbf{E}^p$), $\Delta\phi$ is their phase difference, and ψ is a possible additional phase shift introduced by the detection setup. The true MO response of the system is the figure of merit S_{MO}, i.e., the value of Σ_{MO} for a unit excitation intensity. This quantity can be expressed as a function of the complex reflection and transmission coefficients of the whole structure, which we write in the general form $\rho = re^{i\phi}$ and $\tau = te^{i\varphi}$. For instance, denoting by E^{ss} and E^{pp} the amplitudes of the s and p components of the reflected light electric field for an s excitation of amplitude E_0^s, the complex reflection coefficients ρ^{ss} and ρ^{ps} for these two components are defined by $E^{ss} = \rho^{ss}E_0^s$ and $E^{ps} = \rho^{ps}E_0^s$. In this case, S_{MO} is given by

$$S_{MO} = 2r^{ss}(\theta)r^{ps}(\theta)\cos[\Delta\phi^{ps}(\theta) + \psi], \qquad (2)$$

where $\Delta\phi^{ps} = \phi^{ss} - \phi^{ps}$. Similar expressions hold for p excitation with permutation of the superscripts s and p. For transmission measurements, the reflection coefficients must be simply changed into the transmission coefficients.

According to Eq. (2) (and equivalent expressions), for each incident polarization, S_{MO} depends on three physical quantities. Three measurements are then necessary to analyze the MO signal. We have performed such a precise analysis of the reflected beam in a wide range of incidence angles, for both incident polarizations (Fig. 2). We first measured the reflectivity [i.e., the dc detector output signal normalized over the incident intensity, curves
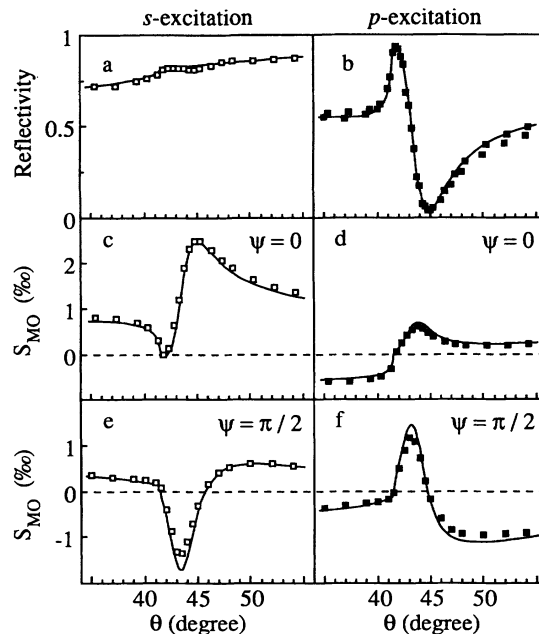

FIG. 2. Variation with the incidence angle θ of the reflectivity (a) and (b) and the MO figure of merit S_{MO} (c)-(f) of the Au/Co/Au sample. The left column (a), (c), and (e) correspond to s excitation and the right column (b), (d), and (f) to p excitation. The MO signal is measured in the reflected beam with a linear-light analyzer (c) and (d) and with a circular-light analyzer (e) and (f). The symbols represent the experimental points and the full lines are the theoretical fits.

in Figs. 2(a) and 2(b)], the square root of which directly gives r^{ss} and r^{pp}. For p excitation [Fig. 2(b)], the pronounced minimum characteristic of the excitation of the gold surface plasmon [5] is observed at the resonance angle $\theta_R \approx 44.5°$. We then performed two sets of measurements of the MO signal. One is obtained with only the linear-polarization analyzer [curves in Figs. 2(c) and 2(d)], which corresponds to $\psi = 0$; the other is obtained by adding a quarter-wave plate oriented at 45° to the linear-polarization analyzer [curves in Figs. 2(e) and 2(f)], which corresponds to $\psi = \pi/2$. The variations with θ of the relevant MO quantities $\Delta\phi^{ps}$, $\Delta\phi^{sp}$, r^{ps}, and r^{sp} [10], straightforwardly deduced from these measurements, are plotted in Fig. 3.

In the total reflection range ($\theta > 41.5°$), for both s and p excitations, the MO effect exhibits, in the vicinity of θ_R, a remarkable feature typical of resonance behavior: $\Delta\phi^{ps}$ and $\Delta\phi^{sp}$ vary by almost π, while r^{ps} and r^{sp} are strongly enhanced. For s excitation, this structure corresponds to a MO figure of merit about 3 times larger than the one obtained in the standard reflection geometry (i.e., in nontotal reflection condition).

We have developed a theory for magneto-optics of a few monolayers thick magnetic medium (Co) embedded in a nonmagnetic metallic matrix (Au), which accounts for the nonlocality of the Co dielectric tensor together with the Au surface plasmon and uses the Green functions method [11]. We obtained this way all the theo-

retical curves plotted in Figs. 2 and 3 (full lines), which fit to the experimental data for the following values of the dielectric constants: in gold $\varepsilon_2 = -11 + 2i$, in cobalt $\varepsilon_a = -11.5 + 18.3i$ (the diagonal elements of the dielectric matrix), and $\varepsilon_b = 0.65i$ (the off-diagonal elements of the dielectric matrix). These values are close to those generally quoted in the literature [12]. The predictions of the model can also be obtained from straightforward but tedious matrix calculations, which account for both the Fresnel electrodynamical boundary conditions and the tensor character of the dielectric constant in the magnetic

medium [13]. In order to get a physical insight into the problem, we discuss here the analytical expressions for the MO coefficients of the whole system, obtained from this calculation, to first order in ℓ. In these expressions we use the complex "reflection coefficients" ρ and "transmission coefficients" τ of the two light electric field components, as indicated by the superscripts s or p, at the different interfaces between two adjacent media designated by double-number subscripts where 1 refers to glass, 2 to gold, and 3 to air. As an example ρ^{ps} is given, in this framework, by

$$\rho^{ps} = \frac{k_2 \varepsilon_b \ell}{2\varepsilon_2 \cos\theta} \frac{e^{ik_2 d'} \tau_{12}^s (1 + \rho_{23}^s e^{2ik_2 d''})}{1 + \rho_{12}^s \rho_{23}^s e^{2ik_2 d}} \frac{e^{ik_2 d'} \tau_{21}^p (1 + \rho_{23}^p e^{2ik_2 d''})}{1 + \rho_{12}^p \rho_{23}^s e^{2ik_2 d}}, \tag{3}$$

where k_2 is the complex z component of the light wave vector in medium 2 (gold).

The first factor of Eq. (3) is the $s \rightarrow p$ conversion factor in the Co layer. It is proportional to ε_b, i.e., to the magnetization. The second factor is the expression for the total s-excitation amplitude in the Co layer. The third factor describes the propagation and interface transmission, between the Co layer and the observation in glass, of the p-wave magneto-optically generated in the Co layer. Both the second and third factors account for multiple reflections at the Au/air and Au/glass interfaces. The plasmon resonance arises here through ρ_{23}^p, in the numerator of the third factor (the denominator term involving ρ_{23}^p is attenuated), which shows a strong amplitude enhancement and phase variation around θ_R.

For p excitation, the $p \rightarrow s$ conversion factor is $\varepsilon_b \ell k_0^2 \cos\theta / 2k_2$, and ρ^{sp} is obtained by exchanging the superscripts s and p in the second and third factor of Eq. (3). One can verify that $\rho^{sp} = \rho^{ps}$ and consequently that $r^{sp} = r^{ps}$, which is experimentally observed (Fig. 3) [14]. It is now the second factor, describing the total p-excitation amplitude in the Co layer, which contains the resonant quantity ρ_{23}^p in exactly the same form as ρ^{ps}.

Thus, for any incident light polarization, the p component of the electric field, either magneto-optically induced or from the excitation, couples with the gold surface plasmon at the Au/air interface, giving rise to a resonant feature in both ρ^{sp} and ρ^{ps}.

Another way to describe the resonant coupling of the gold surface plasmons with the p component of the light electric field is to regard it as an accumulation, at the sample surface, of the corresponding light energy. This should result in an amplified p component of the evanescent electric field [5]. We demonstrated this effect by measuring, versus θ, the evanescent mode intensities I^p and I^s collected in near-field, with the tip at the same distance from the sample surface, respectively, for p- and s-polarized incident light of the same intensity. In Fig. 4(a) we present, as a function of θ, the experimental values (symbols) of the ratio I^p / I^s normalized to I^p / I^s measured on the bare prism [9]. This plot shows the resonant behavior of I^p which is almost 100 times larger than I^s at θ_R.

Correspondingly, the MO signal in the evanescent mode also features this p-wave amplification. Indeed, to first order in ℓ, the transmission coefficient τ^{ps} (p observation in air, under s excitation), for instance, contains the first two factors of Eq. (3), the third factor being replaced by
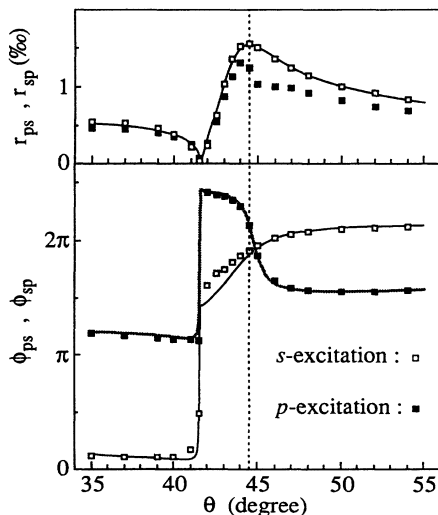

FIG. 3. Variation with the incidence angle θ of the MO reflection coefficient for s and p excitations: the amplitude (r_{ps} and r_{sp}) and the phase difference ($\Delta\phi_{ps}$ and $\Delta\phi_{sp}$). The symbols represent the experimental determinations and the full lines are the theoretical fits (which are identical for r_{ps} and r_{sp}). The vertical dotted line indicates the resonance incidence angle θ_R. The singularities of both $\Delta\phi$ and r, at $\theta = 41.5°$, correspond to the total reflection limit.

$$-\frac{\sqrt{\varepsilon_3}\cos\theta}{\sqrt{\varepsilon_3 - \varepsilon_1 \sin^2\theta}} \frac{e^{ik_2 d''} \tau_{23}^p (1 + \rho_{21}^p e^{2ik_2 d'})}{(1 + \rho_{12}^p \rho_{23}^p e^{2ik_2 d})}, \tag{4}$$

which evidences the resonance due to the transmission coefficient τ_{23}^p of the p wave at the gold/air interface. In Fig. 4(b), we present three sets of near-field measurements, for s excitation [15], of the variation with θ of Σ_{MO} normalized over the total collected intensity I^s [$\Sigma_{MO}/I^s = (t^{ps}/t^{ss})\cos(\Delta\varphi^{ps} + \psi)$]. They are obtained
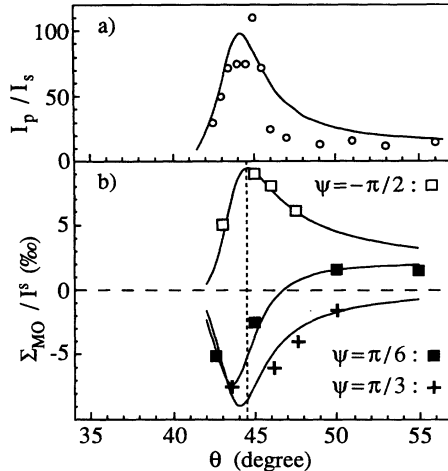
FIG. 4. Variation with the incidence angle θ of (a) the ratio I^p/I^s of the evanescent mode intensities measured for p and s excitations (b) Σ_{MO}/I^s the MO signal measured in the evanescent mode for s excitation, normalized to the total collected intensity. The symbols represent the measurements and the full lines are the theoretical fits. The experimental values of Σ_{MO} are obtained for three different fiber configurations. The theoretical variations match the three sets of measurements accounting for the three indicated values of the additional phase shift ψ induced by the fiber. The vertical dashed line indicates the resonance incidence angle θ_R.

with three different fiber configurations which introduce three different values of the additional retardation ψ. The theoretical curves (full lines), obtained using the complete model, match the three experimental data sets (symbols) when we use the above set of optical constants and suitable values of ψ accounting for the different fiber configurations. On each of the three curves, the amplification of the near-field MO response is observed at resonance.

The experimental and theoretical results presented here demonstrate that in total reflection geometry, the intense and sharp surface plasmon resonances of noble metals can strongly increase the MO figure of merit in noble-metal/ferromagnetic-metal multilayer systems, already known to exhibit large MO response. Moreover, in the Au/Co/Au thin film that we have studied, the MO signal in the evanescent field reaches, at resonance, nearly 1% of the total collected intensity, for a single 1 nm thick ferromagnetic layer. This could provide a significant advantage to high-resolution near-field optical imaging of submicronic magnetic domains [9,16], in particular for technological applications such as high-density data storage.

*Permanent address: A. F. Ioffe Physico-Technical Institute, 194021 Saint Petersburg, Russia.

[1] E. Vélu et al., Phys. Rev. B 37, 668 (1988); M. N. Baibich et al., Phys. Rev. Lett. 61, 2472 (1988); J. Ferré et al., Appl. Phys. Lett. 56, 1588 (1990).

[2] T. Katayama et al., Phys. Rev. Lett. 60, 1426 (1988); W. A. McGahan et al., Appl. Phys. Lett. 55, 2479 (1989); J. Ferré, in Proceedings of the Conference on Magnetism, Magnetic Materials and their Applications, La Habana, Cuba, 1991 (IOP Publishing Ltd, Berkshire, 1992).

[3] H. Feil and C. Haas, Phys. Rev. Lett. 58, 65 (1987).

[4] J. Schoenes and W. Reim, Phys. Rev. Lett. 60, 1988 (1988); H. Feil and C. Haas, Phys. Rev. Lett. 60, 1989 (1988); R. Nies and F. R. Kessler, Phys. Rev. Lett. 64, 105 (1990); T. Katayama et al., Phys. Rev. Lett. 64, 106 (1990).

[5] H. Raether, in Springer Tracts in Modern Physics (Springer-Verlag, Berlin, 1988), Vol. 11.

[6] P. E. Fergusson, O. M. Stafsudd, and R. F. Wallis, Physica (Amsterdam) B89, 91 (1977).

[7] C. Marlière, D. Renard, and J. P. Chauvineau, Thin Solids Films 201, 317 (1991), and references therein.

[8] D. Courjon, K. Sarayeddine, and M. Spajer, Optics Commun. 71, 23 (1989); R. C. Reddick et al., Rev. Sci. Instrum. 61, 3669 (1990).

[9] V. I. Safarov et al., in Proceedings of the Second Near-Field Optics Conference (NFO2), Raleigh, 1993 (to be published).

[10] Kerr rotation and ellipticity, which are commonly considered in MO studies, can be straightforwardly deduced from the quantities that we measure: They are, respectively, the real part and the imaginary part of $(-\rho^{sp}/\rho^{pp})^*$ or ρ^{ps}/ρ^{ss} [J. Zak et al., Phys. Rev. B 43, 6423 (1991)]. Here, we do not discuss these Kerr effect characteristics since in our case they may exhibit "apparent enhancement" due to the strong variation of reflectivity (i.e., of ρ^{pp}) at resonance.

[11] A detailed report of the present theoretical treatment will be published elsewhere. It is a magneto-optical generalization of the following work: V. A. Kosobukin, Zh. Tekh. Fiz. 56, 1481 (1986) [Sov. Phys. Tech. Phys. 31, 879 (1986)].

[12] S. Visnovsky et al., J. Magn. Magn. Mater. 128, 179 (1993).

[13] J. Zak et al., J. Magn. Magn. Mater. 89, 107 (1990); V. M. Agranovich, in Surface Polaritons, edited by V. M. Agranovich and D. L. Mills (North-Holland, Amsterdam, 1982), p. 187.

[14] The experimental determination of r_{sp} is less precise than that of r_{ps} because of the low value of the reflectivity at resonance for p excitation.

[15] In contrast to I^p, the total evanescent intensity I^s collected close to the gold surface varies smoothly with θ. The variation with θ of Σ_{MO}/I^s is practically equivalent to that of the near-field magneto-optical figure of merit.

[16] E. Betzig et al., Appl. Phys. Lett. 61, 142 (1992).